Essential diurnal Rac1 activation during retinal phagocytosis requires αvβ5 integrin but not tyrosine kinases focal adhesion kinase or Mer tyrosine kinase

Yingyu Mao and Silvia C. Finnemann
Department of Biological Sciences, Fordham University, Bronx, NY 10458

ABSTRACT **Diurnal phagocytosis of shed photoreceptor outer-segment particles by retinal pigment epithelial (RPE) cells belongs to a group of conserved clearance mechanisms employing αv integrins upstream of tyrosine kinases and Rho GTPases. In this study, we tested the interdependence of the tyrosine kinases focal adhesion kinase (FAK) and Mer tyrosine kinase (MerTK) and Rho GTPases during engulfment. RPE cells activated and redistributed Rac1, but not RhoA or Cdc42, during phagocytosis. Toxin B, overexpression of dominant-negative Rac1, or decreasing Rac1 expression prevented particle engulfment. Fluorescence microscopy showed that Rac1 inhibition had no obvious effect on F-actin arrangement in resting RPE but prevented recruitment of F-actin to surface-bound phagocytic particles. Quantification of active GTP-Rac1 in wild-type and mutant RPE in culture and in vivo revealed that Rac1 activation during phagocytosis requires αvβ5 integrin and its ligand milk fat globule EGF factor-8 (MFG-E8) but not the receptor tyrosine kinase MerTK. Abolishing tyrosine kinase signaling downstream of αvβ5 toward MerTK by inhibiting FAK specifically or tyrosine kinases generally neither prevented Rac1 activation nor F-actin recruitment during phagocytosis. Likewise, inhibiting Rac1 had no effect on FAK or MerTK activation. We conclude that MerTK activation via FAK and F-actin recruitment via Rac1 both require MFG-E8–ligated αvβ5 integrin. Both pathways are independently activated and required for clearance phagocytosis.**

Monitoring Editor
Carole Parent
National Institutes of Health

Received: Oct 7, 2011
Revised: Jan 9, 2012
Accepted: Jan 13, 2012

INTRODUCTION

Swift and efficient clearance phagocytosis, also called efferocytosis, is a critical aspect of tissue homeostasis. Every day, 0.5–1% of cells in mammals undergo cell death by apoptosis as part of normal tissue renewal. Removal by phagocytosis of the resulting billions of apoptotic cells is necessary to prevent debris buildup, needless activation of inflammatory pathways, and autoimmune disease. Uptake may be accomplished by professional phagocytes, such as macrophages, or by most bystander cells, including fibroblasts and epithelial cells. Mechanistically, clearance phagocytosis is a two-step process. Tethering of apoptotic cells or particles to cell surface receptors, including αv integrins on phagocytic cells, causes tyrosine kinase signaling, RhoA family GTPase activation (specifically of Rac1 and/or Cdc42), and recruitment and rearrangement of F-actin beneath tethered particles (for recent reviews, please see Dupuy and Caron, 2008; Erwig and Henson, 2008). Interfering with integrin recruitment of cytoplasmic proteins, tyrosine kinase signaling, or GTPase activation inhibits particle engulfment, as shown by numerous studies of uptake of apoptotic cells by various mammalian cells in culture (Albert *et al.*, 2000; Leverrier and Ridley, 2001; Tosello-Trampont *et al.*, 2001; Akakura *et al.*, 2004; Wu *et al.*, 2005; Nakaya *et al.*, 2006). Integrin overexpression increases both binding and engulfment steps of clearance phagocytosis, as well as protein

This article was published online ahead of print in MBoC in Press (http://www.molbiolcell.org/cgi/doi/10.1091/mbc.E11-10-0840) on January 19, 2012.

Address correspondence to: Silvia C. Finnemann (finnemann@fordham.edu).

Abbreviations used: $\beta5^{-/-}$, β5 knockout; β-gal, β-galactosidase; DMSO, dimethyl sulfoxide; DN-Rac, dominant-negative mutant Rac1N17; FAK, focal adhesion kinase; FBS, fetal bovine serum; FcγR, IgG-specific Fc receptor; FITC, fluorescein isothiocyanate; FRNK, FAK-related nonkinase; HBSS, Hank's balanced saline solution; Ig, immunoglobulin; MEF, mouse embryonic fibroblast; MerTK, Mer tyrosine kinase; MFG-E8, milk fat globule EGF factor-8; PBS-CM, phosphate-buffered saline with 0.1 mM $CaCl_2$ and 1 mM $MgCl_2$; POS, photoreceptor outer-segment fragments; PY beads, antiphosphotyrosine beads; RCS, Royal College of Surgeons; RPE, retinal pigment epithelium; siRNA, small interfering RNA; TAM, Tyro3/Axl/Mer; wt, wild type.

tyrosine phosphorylation and Rac1 activity independent of phagocytic stimulus (Albert *et al.*, 2000; Akakura *et al.*, 2004). However, the precise causal relationships of integrins, tyrosine kinases, and GTPase signaling during clearance phagocytosis and their in vivo significance have yet to be elucidated.

A special form of clearance phagocytosis takes place in the mammalian retina. In a synchronized burst of uptake activity, retinal pigment epithelial (RPE) cells remove photoreceptor outer-segment fragments (POS) shed once a day by rod-and-cone neurons in a circadian rhythm. As RPE cells are postmitotic in the mammalian eye, each individual RPE cell must engulf numerous POS every day like clockwork for life. Any imbalance in POS phagocytosis by RPE cells causes debris buildup over time, ultimately harming photoreceptors and causing blindness. Shed POS expose similar "eat me" signals as apoptotic cells, resulting in opsonization with the secreted integrin ligand milk fat globule-EGF8 (MFG-E8; Nandrot *et al.*, 2007). Like other forms of clearance phagocytosis, POS clearance proceeds by engagement of αv integrin receptors (specifically αvβ5; Finnemann *et al.*, 1997; Nandrot *et al.*, 2004), activation of tyrosine kinases (αvβ5-associated focal adhesion kinase [FAK] and cell surface Mer receptor tyrosine kinase [MerTK] have been identified to date; Feng *et al.*, 2002; Finnemann, 2003), and recruitment of F-actin in a classical phagocytic cup (Chaitin and Hall, 1983). Rho family GTPases involved in RPE phagocytosis have not yet been specified.

In this study, we explored POS clearance by RPE cells to unravel the molecular pathway that connects particle recognition by phagocyte cell surface receptors to the formation of the F-actin–rich phagocytic cup. We first identified Rac1 activation specifically as essential for POS phagocytosis and for recruitment of F-actin to surface-bound particles by RPE cells in culture. Taking advantage of the synchronicity of RPE phagocytosis, we quantified GTPase activation with phagocytosis in intact retina of wild-type (wt) and mutant animal models to show that Rac1 activation during POS phagocytosis in vivo requires αvβ5 integrin and its physiological ligand MFG-E8 but not MerTK receptors. Assays of POS uptake by RPE cells in culture confirmed the in vivo findings and further revealed that inhibition of FAK specifically or incubation with tyrosine kinase inhibitors has no effect on Rac1 activation or on recruitment of F-actin to MFG-E8-αvβ5–bound particles. Just as Rac1 activity was unperturbed by inhibition of FAK or MerTK, FAK and MerTK activation occurred normally, even when Rac1 was inhibited. Taken together these results demonstrate that particle binding to αvβ5 integrin of RPE phagocytes initiates two separate downstream signaling pathways, stimulating MerTK via FAK and stimulating Rac1, respectively. F-actin recruitment to the phagocytic cup requires Rac1 but, surprisingly, is independent of tyrosine kinases, including FAK and MerTK.

RESULTS

POS phagocytic challenge of RPE cells in culture activates and relocalizes specifically Rac1

To determine which Rho GTPase family members contribute to RPE phagocytosis, we first tested whether POS particle challenge induced changes in GTPase activity in RPE cells. We used the immortalized RPE-J cell line for these assays, which provides a source of unlimited numbers of highly phagocytic cells that employ the αvβ5-FAK-MerTK phagocytic pathway to take up POS, similar to primary RPE or RPE in the retina (Finnemann *et al.*, 1997; Finnemann, 2003). Pulldown assays with GTPase effector–coated beads showed that RPE-J cells responded to POS incubation, but not to assay medium alone, by increasing the amount of GTP-bound Rac1 (Figure 1A, center). Although RhoA and Cdc42 could be loaded with GTP-γS, such as Rac1 in control samples (Figure 1A, samples denoted by asterisk),

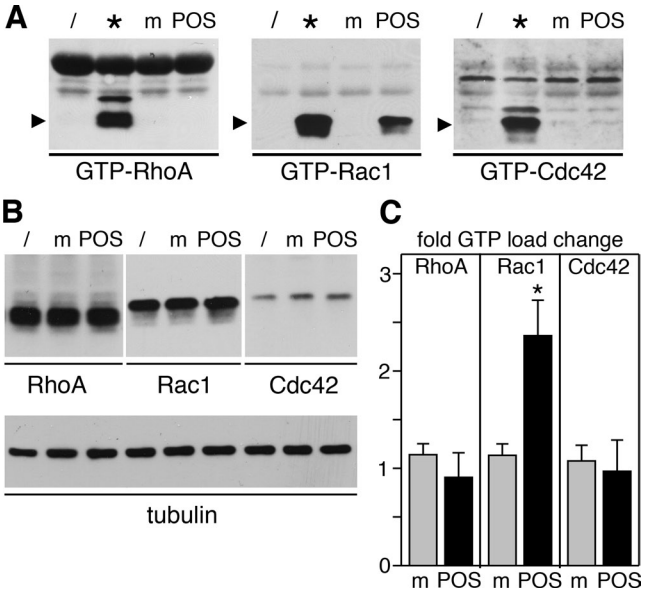

FIGURE 1: POS phagocytic challenge activates Rac1 but not RhoA or Cdc42. RPE-J cells were untreated (/) or were fed with POS (lanes POS) or assay medium (m) for 1 h and were lysed before pulldown affinity isolation of GTP-bound GTPases. Twenty percent of lysates were incubated with GTP-γS as positive control for pulldown procedures (*). GTP-RhoA, GTP-Rac1, or GTP-Cdc42 (A) as well as total GTPases (B) were quantified by immunoblotting, as indicated. Data from one representative of three independent experiments performed are shown. Blot membranes shown in (B) were reprobed to detect tubulin, demonstrating that equal numbers of cells were analyzed in each sample. (C) As an alternate method of GTP-load detection, the same experiment was repeated and analyzed by G-LISA. Data presented are fold change compared with untreated cells in GTP load of RhoA, Rac1, or Cdc42 (as indicated) upon feeding with medium (gray bars) or POS (black bars). Bars show mean ± SD of three independent experiments, each with triplicate samples. Asterisks indicate significant difference compared with untreated cells ($p < 0.05$).

their GTP load did not change with medium or POS incubation (Figure 1A, left and right panels). Protein levels of RhoA, Rac1, and Cdc42 remained unchanged with POS challenge (Figure 1B). G-LISAs provide an alternative to pulldown assays by also quantifying GTPase GTP load while using significantly fewer cells per sample. G-LISAs confirmed that POS challenge significantly increased GTP-Rac1 content of RPE-J cells by 2.4-fold on average but did not significantly change GTP load of RhoA or Cdc42 (Figure 1C). We next investigated Rac1 subcellular distribution in RPE-J cells phagocytosing POS. Immunofluorescence microscopy revealed that Rac1 redistributed to POS phagosomes in RPE-J cells after feeding POS for 1–5 h (Figure 2). At each time point, Rac1 labeled many POS, but not all, suggesting it may localize to a subset of POS phagosomes (e.g., of specific maturation stage). In addition to colocalizing with POS phagosomes, Rac1 retained localization in the cell periphery. In similar experiments investigating RhoA, we did not observe RhoA colocalization with POS phagosomes at any time point (Figure 2, RhoA; unpublished data. Thus, of the three GTPases tested, only Rac1 increases its specific activity and redistributes with POS phagocytosis.

Inhibiting Rac1 or reducing Rac1 expression blocks POS internalization by RPE cells

To test whether Rac1 activation was functionally relevant for the phagocytic process itself, we used a recombinant adenovirus

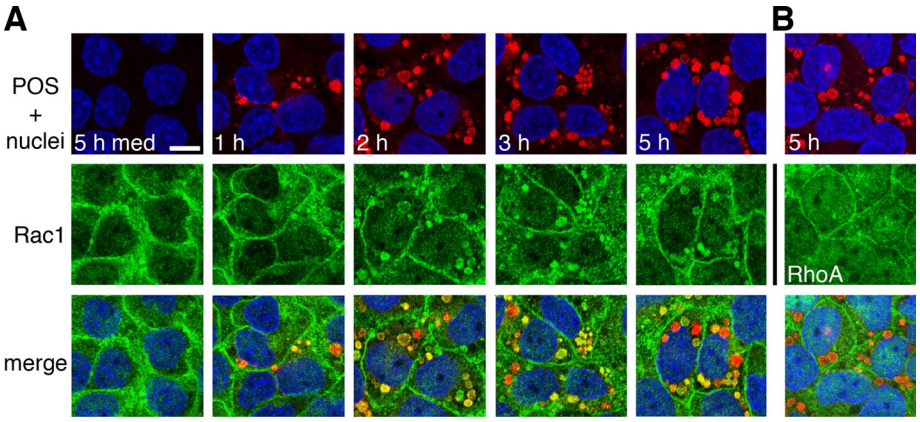

FIGURE 2: Rac1 redistributes to colocalize with phagocytosed POS. RPE-J cells on glass coverslips were challenged with medium for 5 h (5 h med) or with Texas red–stained POS for different lengths of time (as indicated) before immunolabeling of Rac1 (A) or RhoA (B). Single *x-y* confocal scans show: top, overlay of POS (red) with RPE nuclei (blue); middle, GTPases (green); or bottom, overlay of POS, nuclei, and GTPase. Scale bar (for all fields): 10 μm.

expressing a well-characterized point mutant of Rac1, Rac1N17, to prevent Rac1 activation in RPE cells. Rac1N17 is permanently GDP-bound and acts as a dominant-negative mutant (DN-Rac) by blocking the binding of endogenous Rac1-GDP to guanidine nucleotide exchange factors (Ridley *et al.*, 1992). When viewed by fluorescence microscopy, it was immediately obvious that RPE-J cells took up fewer fluorescein isothiocyanate (FITC)-labeled POS during 3.5 h of POS challenge when the cells expressed DN-Rac than when the cells expressed β-galactosidase (β-gal), a control protein also expressed by adenovirus infection (Figure 3, A and B). Quantification of internalized POS by fluorescence scanning revealed that cells expressing DN-Rac internalized on average 73% fewer POS than cells expressing β-gal (Figure 3, C and D). Cells infected with recombinant β-gal adenovirus internalized POS-like uninfected control cells. Selective inhibition of RhoA by incubation with C3 transferase had no significant effect on POS internalization. In contrast, incubation with *Clostridium difficile* toxin B, a universal Rho family GTPase inhibitor, decreased POS internalization to an extent similar to DN-Rac (Figure 3, C and D). Furthermore, silencing Rac1 expression, which caused a specific decrease by 78% on average in Rac1 protein, was sufficient to diminish POS internalization (Figure 3, E–G). These results suggest that among Rho family GTPases, Rac1 specifically is required for POS internalization.

DN-Rac prevents F-actin recruitment to surface-bound phagocytic particles

As Rac1 GTPase activity modulates F-actin dynamics, we next sought to study the effect of DN-Rac on the actin cytoskeleton during POS phagocytosis. F-actin–rich microvilli at the apical, phagocytic surface are considerably less abundant in RPE-J cells than in RPE in the eye (Bonilha *et al.*, 1999). Therefore we investigated the effects of DN-Rac on POS uptake by rat primary RPE cells excised from eyecups in patches and grown in culture without passaging. These cells retain the F-actin arrangement of the RPE in the eye (Bonilha *et al.*, 1999). To determine whether DN-Rac affected POS internalization by primary RPE in a manner similar to RPE-J cells, we used a pulse–chase protocol to separate POS binding from POS engulfment. During an initial pulse with excess POS at 20°C, RPE cells bind POS via αvβ5 integrin, but their rate of internalization is considerably less than at normal growth temperature (Finnemann and Rodriguez-Boulan, 1999). We incubated primary RPE expressing β-gal or DN-Rac with POS at 20°C for 1 h. We distinguished bound from internalized particles by washing cells after POS challenge before lysis with EDTA-containing buffer, which removes integrin-bound particles (Akakura *et al.*, 2004). Immunoblot analysis of cells washed and lysed after this pulse did not show significant differences in total (surface-bound plus internal) or in internal POS between cells expressing DN-Rac and β-gal (Figure 4, A and B, pulse). For parallel samples, we removed unbound POS after the pulse and continued incubation at 37°C for 30 min. During this chase period, cells expressing β-gal internalized significantly more POS than cells expressing DN-Rac: immunoblotting for the POS marker opsin showed 70% less internal POS after the chase when comparing absolute POS-opsin between cells expressing DN-Rac and β-gal (Figure 4, A and B, chase). This also resulted in a significantly smaller relative fraction of internal POS in DN-Rac–expressing cells: 41% compared with 71% in β-gal–expressing cells (Figure 4C). Immunoblotting confirmed that primary RPE cells were efficiently transduced (Figure 4A, β-gal, Rac1, RPE65 as loading control). Thus Rac1 inhibition affects primary rat RPE in a manner similar to RPE-J cells, specifically decreasing POS internalization. We now repeated the pulse–chase POS phagocytosis experiment on primary RPE expressing DN-Rac or β-gal and costained with POS-opsin antibodies and the F-actin–binding drug phalloidin. Figure 5A shows that regardless of exogenous protein expression, cells incubated with assay medium or with POS during the pulse showed abundant cortical F-actin. The same was true for untreated cells (unpublished data). Furthermore, there was no obvious change in F-actin distribution in DN-Rac–expressing or β-gal–expressing cells incubated with medium during pulse and chase (Figure 5B, m). In contrast, β-gal–expressing cells chased for 10 min at 37°C recruited F-actin to sites of bound POS at their apical surface (Figure 5B, left, POS). We did not observe this F-actin recruitment in cells expressing DN-Rac (Figure 5B, right, POS). Thus Rac1 inhibition in RPE cells does not disrupt cortical F-actin but prevents F-actin assembly beneath the bound POS that initiates formation of the phagocytic cups essential for POS engulfment.

Rac1 activation during phagocytosis requires αvβ5 integrin and its ligand MFG-E8 but is independent of MerTK

In clearance phagocytosis, particle tethering to αvβ3/5 integrins is followed by activation of cell surface receptor tyrosine kinases of the Tyro3/Axl/Mer (TAM) family. In the RPE, POS binding to αvβ5 integrin receptors stimulates MerTK activation, which is essential for particle engulfment. To test the surface receptor dependence of Rac1 activation during RPE phagocytosis, we investigated mice lacking αvβ5 integrin ($\beta5^{-/-}$ mice) or its ligand MFG-E8 (MFG-$E8^{-/-}$ mice) and rats lacking MerTK (Royal College of Surgeons [RCS] rats). POS shedding and RPE phagocytosis follows a strict circadian rhythm in mammals, in which the peak of phagocytosis coincides with the daily onset of light. This allows correlatiion of protein activities with phagocytic activity by comparing protein activities between tissues harvested at peak and off-peak phagocytosis times. We harvested eyes from wt and $\beta5^{-/-}$ mice 1 h before and 1 h and 3 h after light onset and tested Rac1 GTP load with G-LISAs. We found that GTP-Rac1 increased 2.3-fold in wt mouse eyes from 1 h before to 1 h after light onset and declined by 3 h (Figure 6A). These changes in Rac1 activity correlate

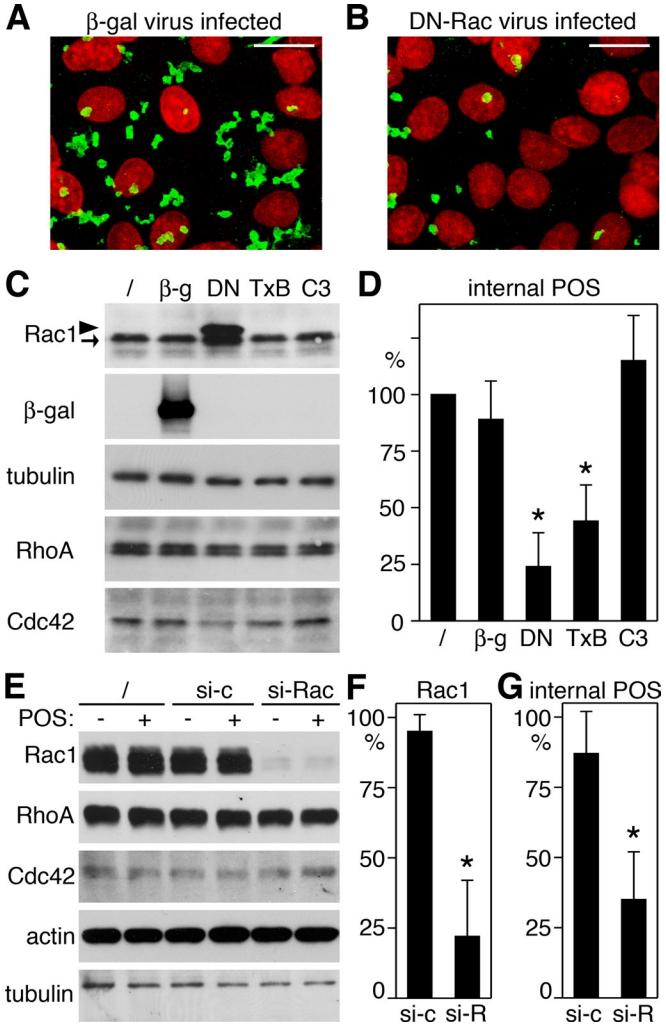

FIGURE 3: DN-Rac, toxin B, or decreasing Rac1 expression inhibit POS phagocytosis. (A and B) RPE-J cells infected with β-gal (A) or DN-Rac (B) encoding adenovirus were challenged with FITC-stained POS for 3.5 h before fixation and fluorescence microscopy of phagocytosed POS (green) and RPE nuclei (red). Representative maximal projections of merged images are shown for three independent experiments performed. Scale bars: 10 μm. (C and D) RPE-J cells infected as above or untreated (/) or treated overnight with toxin B (TxB) or C3 transferase (C3) were fed with POS for 3.5 h. (C) Samples were analyzed by immunoblotting. Rac1 demonstrates similar levels of DN-Rac (arrowhead) and endogenous Rac1 (arrow) in DN-Rac adenovirus–infected cells (DN) and equal levels of Rac1 in all other samples. As expected, β-gal expression was restricted to cells infected with β-gal adenovirus (β-g). All samples contained equal levels of RhoA, Cdc42, and tubulin, which served as loading control. (D) Internalized POS were quantified by fluorescence scanning, as described in *Materials and Methods*. Bars show relative numbers of internalized POS marked as indicated and as in (C) compared with untreated cells (/). (E to G) RPE-J cells were used untreated (/) or incubated with nonspecific control siRNA (si-c) or siRNA specific to Rac1 (si-Rac, si-R) for 2 d before challenge with medium (–) or POS (+) for 3.5 h. (E) Samples were analyzed by immunoblotting to demonstrate specific decrease in Rac1 protein in cells treated with siRNA to Rac1. (F) Bars show relative levels of Rac1 protein as compared with untreated cells. (G) POS internalized by cells characterized in (E) and (F) were quantified as in (D). (D, F, and G) Data are presented as mean ± SD of three independent experiments with triplicate samples each. Asterisks indicate significant difference from untreated cells ($p < 0.05$).

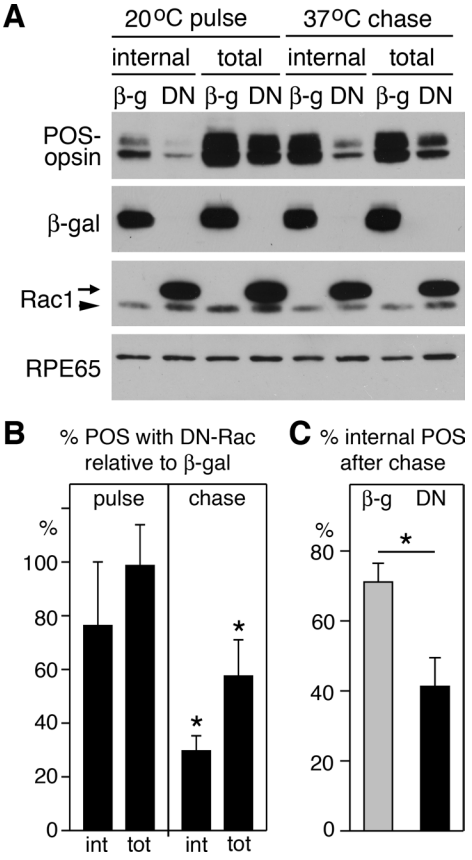

FIGURE 4: DN-Rac specifically inhibits POS internalization. Primary wt rat RPE cells infected with β-gal or DN-Rac encoding adenovirus were used for pulse–chase POS phagocytic challenge before lysis and analysis by immunoblotting and densitometry. POS-opsin blotting revealed similar total (bound plus internal) POS taken up by cells expressing β-gal or DN-Rac (A, 20°C pulse; B, pulse). However, significantly more bound POS were internalized during 30-min chase (A, 37°C chase; B, chase). (A) A representative immunoblot is shown with probes as indicated. For Rac1, arrow indicates DN-Rac; arrowhead indicates endogenous Rac1. (B) Bars report relative total or internal POS taken up by DN-Rac–expressing cells compared with β-gal–expressing cells. (C) Bars report fraction of internalized POS relative to total POS in cells expressing β-gal (gray bar) or DN-Rac (black bar). Data in (B) and (C) show mean ± SD of five independent experiments. Asterisks mark significant differences between DN-Rac–expressing and β-gal–expressing RPE cells ($p < 0.05$).

precisely with peak phagocytosis in the retina. In contrast, we found no change in Rac1 activity at any time point studied in $\beta5^{-/-}$ eyes, in which phagocytosis lacks the diurnal peak (Figure 6A). G-LISA changes reflected changes in specific activity of Rac1, rather than secondary effects, as control immunoblot experiments confirmed equal expression of Rac1, as well as of Cdc42 and RhoA in wt and $\beta5^{-/-}$ tissue at all time points tested (Figure 6B). Furthermore, in phagocytosis assays challenging wt and $\beta5^{-/-}$ primary RPE cells in culture, we confirmed both by GTP-Rac1 pulldown (Figure 6C) and by G-LISA (Figure 6D) that wt RPE cells specifically responded to phagocytic challenge with Rac1 activation, while $\beta5^{-/-}$ RPE cells did not. Differential Rac1 activation of wt and $\beta5^{-/-}$ RPE cells during phagocytic challenge with identical particles made it highly unlikely that Rac1 activation differed in intact retina because of changes in photoreceptor shedding rather than RPE uptake. We sought to further probe the relevance of the αvβ5 pathway for diurnal Rac1

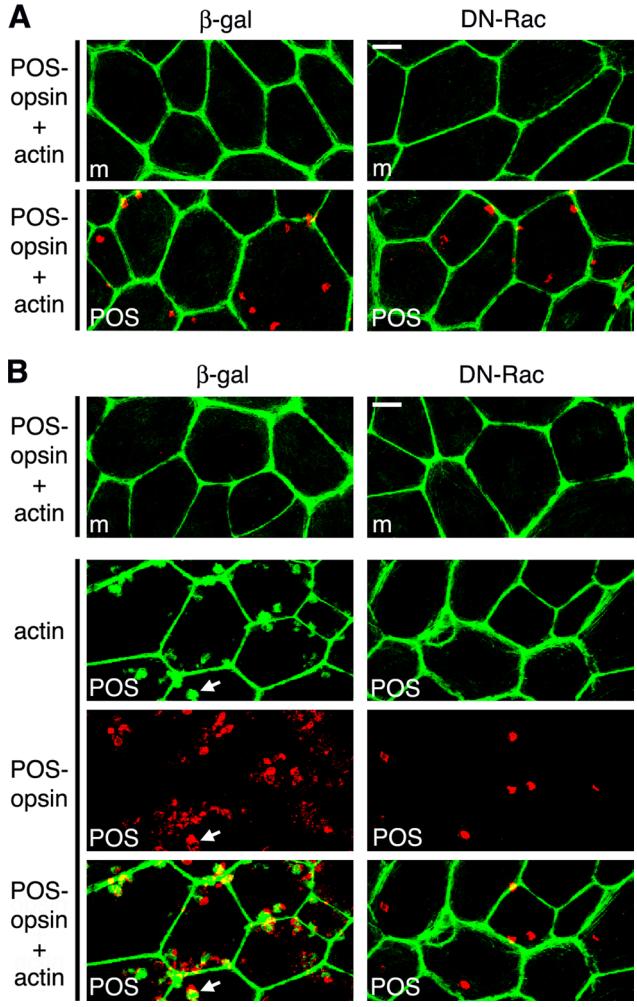

FIGURE 5: DN-Rac inhibits actin recruitment to phagocytic POS particles. Primary wt rat RPE cells infected with β-gal or DN-Rac encoding adenovirus were used for pulse–chase POS phagocytic challenge, as described in *Materials and Methods*, before fixation, fluorescence labeling of POS and F-actin, and analysis by confocal microscopy. All fields show maximal projections. (A) Cells challenged with assay medium (m) or POS were fixed and labeled at the end of the POS pulse. Fields show overlay of POS-opsin (red) and F-actin (green) images. (B) Cells were processed after pulse and 10-min chase. Top, overlay of POS-opsin (red) and F-actin (green) images in cells treated with assay medium during pulse and chase (m). Bottom three panels (POS) show one field for each infection. Separate actin and POS-opsin images, as well as the overlay of both as indicated, are shown. Representative fields of a total of four independent experiments are shown. Arrow indicates an example of F-actin recruited to POS in β-gal–expressing cells. Scale bars: 10 μm.

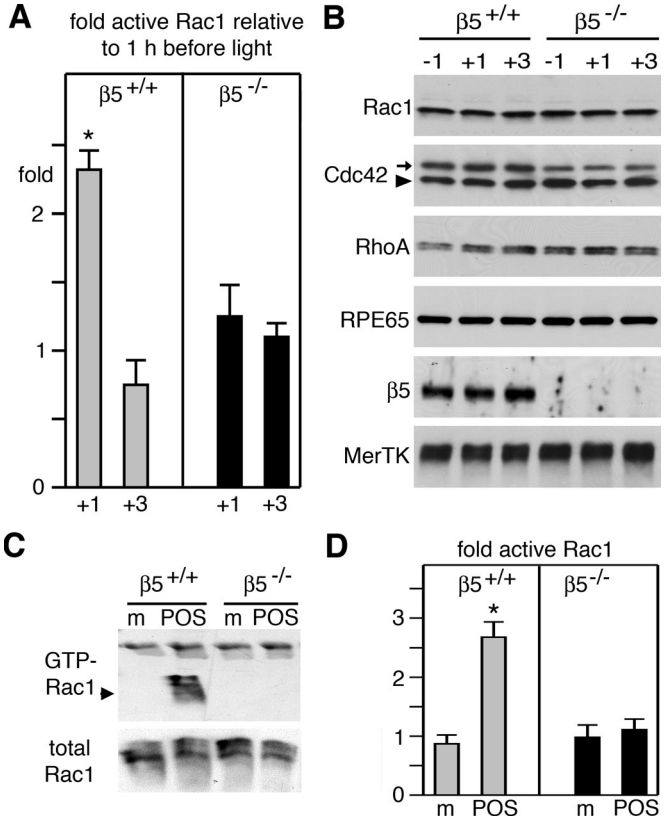

FIGURE 6: Rac1 activity increases at the time of diurnal POS phagocytosis in intact retinal tissue of wt, but not $\beta5^{-/-}$, mice and in primary wt, but not $\beta5^{-/-}$, mouse RPE in culture in response to POS. (A) GTP-Rac1 levels were quantified by G-LISA in eyecups harvested from wt mice (gray bars) and $\beta5^{-/-}$ mice (black bars) 1 h before, 1 h after, or 3 h after light onset. Bars report relative GTP-Rac1 at times after light onset compared with GTP-Rac1 at 1 h before light. Data show mean ± SD of three independent experiments, each analyzing three mice of each genotype. Asterisk denotes significant difference ($p < 0.05$). (B) Immunoblot detection of proteins as indicated in representative G-LISA lysates confirm genotype (β5), lack of protein level fluctuation with time, and equal load (RPE65). Arrowhead in Cdc42 blot indicates Cdc42 (at ~21 kDa); arrow indicates mouse IgG detected in eye tissue by anti–mouse IgG secondary antibody (at ~25 kDa). (C) Immunoblot detection of Rac1 in GTP-Rac1 pulldown assays (GTP-Rac1) and whole lysates (total Rac1) of lysates from primary wt or $\beta5^{-/-}$ RPE (as indicated) following challenge for 30 min with assay medium (m) or POS. (D) Experiments as in (C) were analyzed by G-LISA. Bars report relative GTP-Rac1 compared with GTP-Rac1 in untreated cells. Gray bars show results from wt RPE cells; black bars show results from $\beta5^{-/-}$ RPE cells. Data show mean ± SD of three independent experiments, each testing duplicate samples. Asterisk marks significant change in GTP-Rac1 ($p < 0.05$).

activation by quantifying active Rac1 in eyes of mice with normal expression of αvβ5 receptors but lacking its endogenous ligand MFG-E8. These MFG-E8$^{-/-}$ mice exhibit the same defect in phagocytic rhythm as $\beta5^{-/-}$ mice, while phagocytosis in MFG-E8$^{+/-}$ mice is normal (Nandrot *et al.*, 2007). Figure 7 shows that Rac1-GTP increased significantly after light onset in eyes of MFG-E8$^{+/-}$ mice but not in eyes of MFG-E8$^{-/-}$ mice. Taken together these results show that phagocytosis by RPE in vivo and in culture causes Rac1 activation, and this activation requires αvβ5 integrin and its ligand MFG-E8.

Next we performed the same experiment, this time comparing Rac1 GTP load with time of phagocytosis in wt and MerTK-deficient RCS rat eyes. Between 1 h before and 1 h after light onset, Rac1 activity increased on average by 3.2-fold in wt rat eyes and by 2.5-fold in MerTK-deficient eyes (Figure 8A). The difference in extent of increase was not statistically significant. In wt eyes, GTP-Rac1 declined to baseline levels by 3 h after light onset, while GTP-Rac1 decreased less in RCS eyes, remaining twofold elevated (Figure 8A). At this time, we do not understand this persistence in Rac1 activity. As in mouse tissue, we found no change in relevant protein levels during time of phagocytosis to indicate specific activity increases of Rac1 in rats of both genotypes (Figure 8B). Similar to wt mouse RPE and RPE-J cells, wt rat RPE in culture robustly activated Rac1 upon

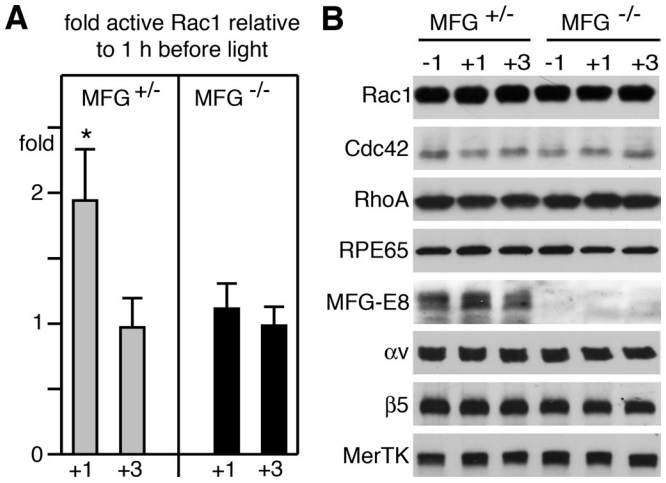

FIGURE 7: Rac1 activity increases at the time of diurnal POS phagocytosis in intact retinal tissue of MFG-E8$^{+/-}$, but not MFG-E8$^{-/-}$, mice. (A) GTP-Rac1 levels were quantified by G-LISA in eyecups harvested from MFG-E8$^{+/-}$ mice (MFG$^{+/-}$, gray bars) and MFG-E8$^{-/-}$ mice (MFG$^{-/-}$, black bars) 1 h before, 1 h after, or 3 h after light onset. Bars report relative GTP-Rac1 at times after light on compared with GTP-Rac1 at 1 h before light onset. Data show mean ± SD of three independent experiments each analyzing three mice of each genotype. Asterisk denotes significant difference ($p < 0.05$). (B) Immunoblot detection of proteins as indicated in representative G-LISA lysates confirm genotype (MFG-E8), lack of protein level fluctuation with time, and equal load (RPE65).

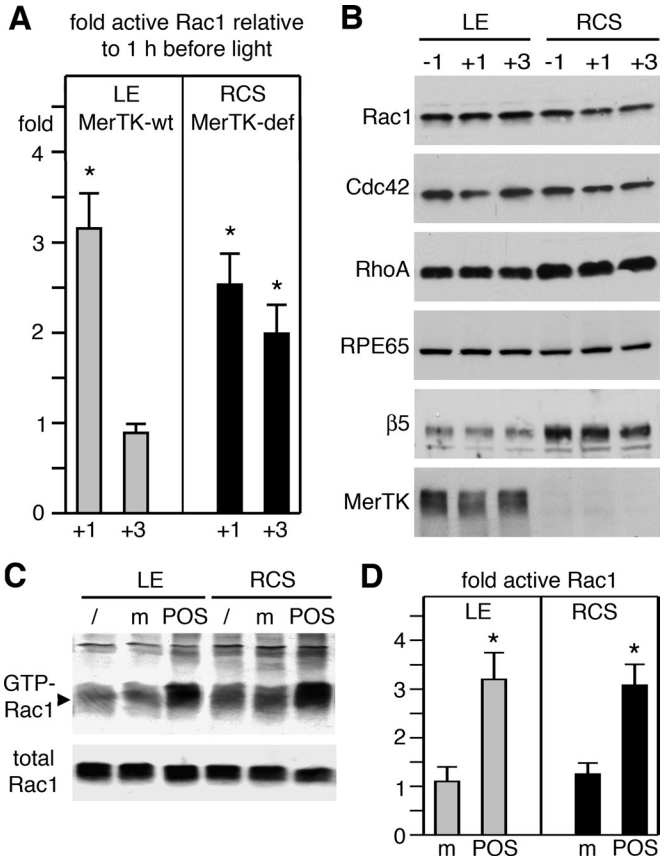

FIGURE 8: Rac1 activity increases at the time of diurnal POS phagocytosis in intact retinal tissue and in primary RPE in culture specifically in response to POS and independently of MerTK expression. (A) GTP-Rac1 levels were quantified by G-LISA in eyecups harvested from wt rats (gray bars) and RCS rats that are MerTK-deficient (MerTK-def, black bars) 1 h before, 1 h after, or 3 h after light onset. Bars report relative GTP-Rac1 at times after light onset compared with GTP-Rac1 at 1 h before light onset. Data show mean ± SD of three independent experiments, each analyzing three rats of each genotype. Asterisks denote significant difference ($p < 0.05$). (B) Immunoblot detection of proteins as indicated in representative G-LISA lysates confirm lack of protein level fluctuation with time and genotype (MerTK). RPE65 served as loading control. (C) Immunoblot detection of Rac1 in GTP-Rac1 pulldown assays (GTP-Rac1) and whole lysates (total Rac1) of lysates from primary wt or RCS RPE (as indicated) that were untreated (/) or challenged for 30 min with assay medium (m) or POS. (D) Experiments as in (C) were analyzed by G-LISA. Gray bars show results from wt RPE cells; black bars show results from RCS RPE cells. Bars report relative GTP-Rac1 compared with GTP-Rac1 in untreated cells. Data show mean ± SD of three independent experiments, each testing duplicate samples. Asterisks mark significant change in GTP-Rac1 ($p < 0.05$).

POS challenge, as shown by GTP-Rac1 pulldown assays (Figure 8C) and by G-LISA (Figure 8D). Strikingly, MerTK-defective RPE responded to phagocytic challenge exactly as did wt RPE (Figure 8, C and D). Thus MerTK-deficient RPE cells activate Rac1 in response to phagocytic challenge, although they cannot engulf particles (Edwards and Szamier, 1977).

Mouse RPE cells express another TAM family receptor, Tyro3, in addition to MerTK (Prasad *et al.*, 2006). We found that Tyro3 immunoblotting showed two bands of similar intensity in RPE-J cells and a similar double band with a far more prominent upper band in RCS RPE cells (Figure 9A). We do not know the relevance of the different bands for protein function, but we conclude that rat RPE cells, similar to mouse RPE cells, express Tyro3. To directly test whether MerTK and/or Tyro3 contribute to Rac1 activation during phagocytosis, we next quantified effects of the TAM ligand Gas6, the αvβ5 ligand MFG-E8 (our standard phagocytosis assay additive), a mix of MFG-E8 and Gas6, and fetal bovine serum (FBS) on GTP-Rac1 levels in response to POS challenge. FBS has been used as standard RPE phagocytosis assay additive for decades, and it contains both integrin and TAM ligands (Edwards and Flaherty, 1986). G-LISAs revealed that POS with Gas6 alone did not increase Rac1 activity of RPE-J cells above levels obtained with serum-free control medium and that MFG-E8 alone raised Rac1 activity to the same extent as a mix of Gas6 and MFG-E8 or FBS (Figure 9B). As in RPE-J cells, Rac1 activity in RCS RPE cells increased when POS were incubated in the presence of MFG-E8, MFG-E8 plus Gas6, or FBS, but not upon addition of Gas6 alone with POS (Figure 9C). Testing effects of the same ligands on POS uptake, we found that Gas6 increased POS uptake by RPE-J cells (albeit less strongly than MFG-E8; Supplemental Figure S1, A and C). As expected, Gas6 had no effect on POS uptake by RCS RPE (Figure S1, B and C). Thus Gas6 was functional as applied in our assays, as it promoted MerTK-dependent phagocytosis. However, Gas6 did not affect Rac1 activity. Taken together these results do not support a role for TAM receptors or their ligand Gas6 in Rac1 activation during POS phagocytosis by RPE cells.

Inhibition of FAK or of tyrosine kinases in general has no effect on Rac1 activation or on F-actin recruitment during phagocytosis

FAK associates with αvβ5 receptors at the apical surface of resting RPE cells, and responds to phagocytic challenge with activation and dissociation from αvβ5 (Finnemann, 2003). Activated FAK is required for subsequent MerTK activation during phagocytosis in vivo and by cells in culture. As FAK activation is independent of MerTK, we

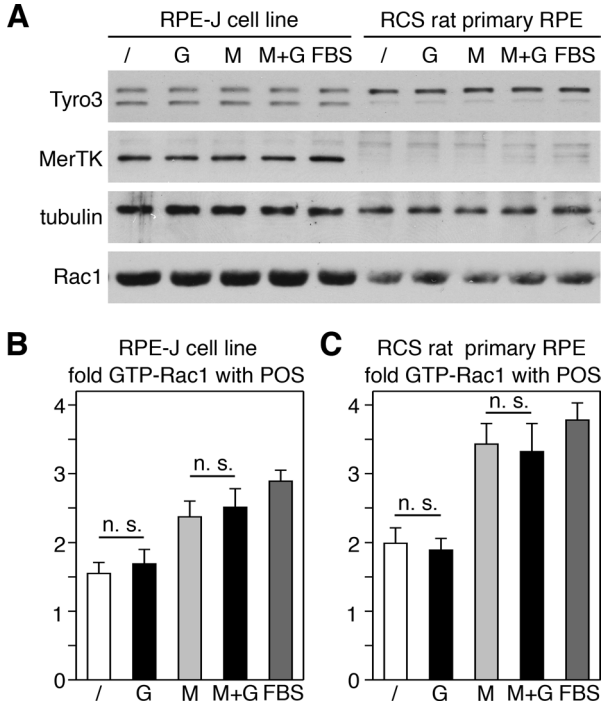

FIGURE 9: Rac1 activation during POS phagocytosis by RPE cells in culture is independent of TAM receptor ligands. RPE-J cells or MerTK-deficient RCS rat primary RPE received POS suspended in DMEM without additives (/) or supplemented with Gas6 (G), MFG-E8 (M), a mix of Gas6 and MFG-E8 (M+G), or FBS (FBS) for 3.5 h or 1.5 h, respectively, before harvest. (A) Immunoblotting of whole-cell lysates showed no differences in TAM receptor or Rac1 protein levels upon challenge with different additives. (B and C) G-LISAs showed that GTP-Rac1 levels of RPE-J (B) and RCS RPE (C) increased to the same extent relative to untreated cells after POS challenge without additives (white bars) or with Gas6 (black bar, G). POS with MFG-E8 alone (light gray bars) raised GTP-Rac1 to the same extent as MFG-E8 plus Gas6 (black bar, M+G). FBS also increased GTP-Rac1 by both cell types (dark gray bar). Bars represent mean ± SD of three independent experiments, each testing duplicate samples; n. s., not significant ($p > 0.1$).

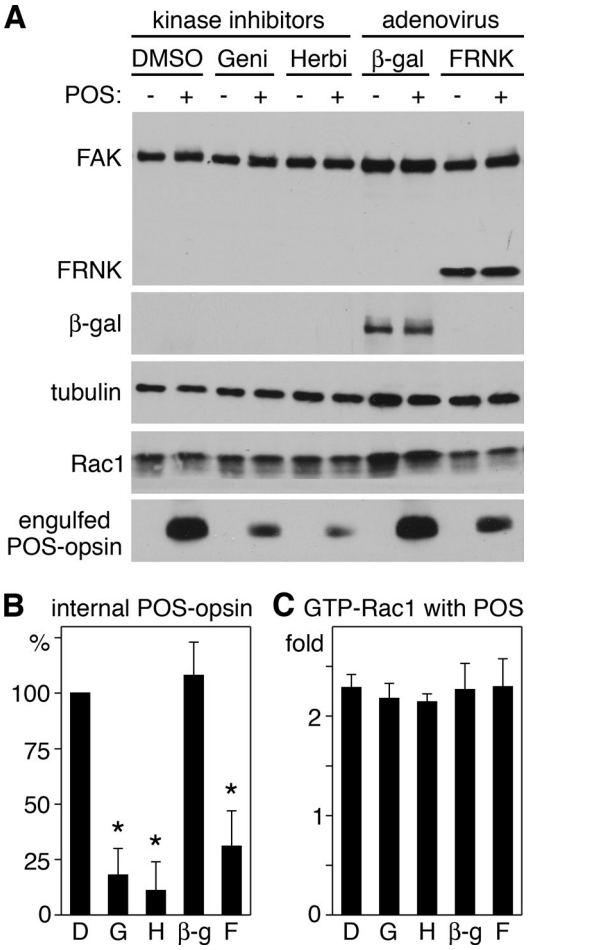

FIGURE 10: Phagocytic challenge activates Rac1 in RPE cells independently of FAK and regardless of presence of tyrosine kinase inhibitors. RPE-J cells were challenged with medium (–) or POS (+) for 3.5 h before lysis. During POS challenge, cells were treated with dimethyl sulfoxide (DMSO) solvent (DMSO), genistein (Geni), or herbimycin A (Herbi) as indicated. Cells expressing adenovirus-encoded β-gal (β-gal) or FRNK (FRNK) were also tested. (A) Whole-cell lysates obtained after EDTA removal of surface-bound POS (as described in *Materials and Methods*) were analyzed by immunoblotting with probes (as indicated). One of three representative experiments is shown. (B) Bars report densitometry quantification of internalized POS of experiments as in (A) normalized to DMSO, which was set at 100%. Data show mean ± SD of three independent experiments. Asterisks mark significant difference compared with DMSO-treated cells ($p < 0.05$). (C) Bars report increase of GTP-Rac1 levels as per G-LISA in cells upon POS challenge compared with the same cells treated with medium. Data show mean ± SD of three independent experiments with triplicate samples for each.

hypothesized that it may relay signals from αvβ5 to Rac1 in a pathway parallel to its activation of MerTK. To test this hypothesis, we inhibited FAK by expressing its fragment, FAK-related nonkinase (FRNK), by adenoviral infection. FRNK acts as a dominant-negative form of FAK, interfering with protein–protein interactions of full-length FAK (Schaller *et al.*, 1993; Sieg *et al.*, 1999). We titrated adenovirus infection to achieve levels of FRNK similar to levels of endogenous FAK in RPE-J cells (Figure 10A). We previously found that this level of FRNK has no direct cytotoxic effects but decreases POS engulfment (Finnemann, 2003). Immunoblotting for POS-opsin confirmed these earlier results, indicating that FRNK expression levels were sufficient to decrease total phagocytosed POS and internal POS (Figure 10, A and B). Unexpectedly, G-LISAs of the same cells found to be defective in engulfment showed normal Rac1 activation in response to POS (Figure 8C). Similarly, broad-spectrum protein tyrosine kinase inhibitors, genistein and herbimycin, failed to diminish Rac1 activation in response to POS (Figure 10C), although they inhibited POS uptake (Figure 10, A and B). To further probe whether FAK was dispensable for Rac1 activation, we quantified changes in GTP-Rac1 in mouse embryonic fibroblasts (MEFs) derived from $FAK^{+/+}$ or from background-matched $FAK^{-/-}$ embryos. We previously found that these MEFs use an integrin-FAK-MerTK–dependent pathway to phagocytose POS (Finnemann, 2003). In this study, $FAK^{+/+}$ and $FAK^{-/-}$ MEFs increased their GTP-Rac1 content to the same extent in response to POS challenge, further supporting the conclusion that FAK is not required for Rac1 activation during POS uptake (Figure S2). To further investigate the functional relevance of these findings, we next tested the effect of FAK or generic protein tyrosine kinase inhibition on F-actin recruitment to surface-bound POS in primary RPE. Immunoblotting confirmed FRNK or β-gal control protein expression, equal levels of Rac1 protein, and a decrease in POS uptake by both FRNK and the drugs (Figure S3). Despite their failure to internalize POS, primary RPE cells expressing FRNK or treated with genistein or herbimycin recruited F-actin to sites of surface-bound

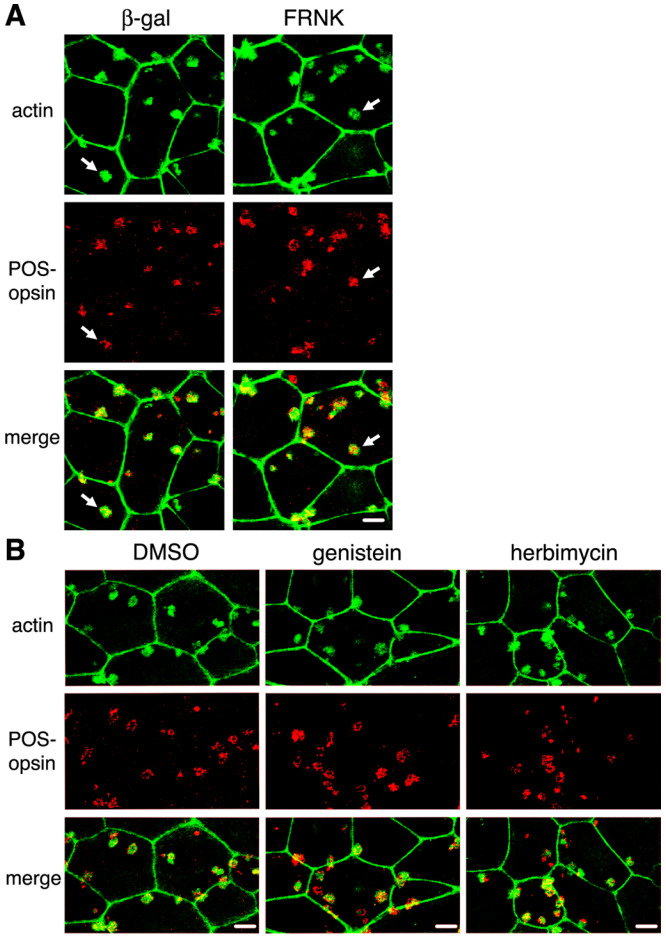

FIGURE 11: Actin recruitment to POS during RPE phagocytosis is unaffected by FRNK or tyrosine kinase inhibitors. Primary wt rat RPE cells were used for pulse–chase POS phagocytic challenge (as described in *Materials and Methods*). Cells were fixed after 10-min chase before fluorescence labeling of POS and F-actin and analysis by confocal microscopy. All fields show maximal projections. For each field: top, F-actin; middle, POS-opsin; bottom, overlay of both. Experiments in (A) and (B) were performed three times each. Scale bars: 10 μm. (A) Images show one representative field each of cells expressing adenovirus-encoded β-gal or FRNK (as indicated). Arrows indicate F-actin recruitment to POS. (B) Images show one representative field each of cells treated with DMSO solvent, genistein, or herbimycin A.

POS-like control cells expressing β-gal or treated with solvent (Figure 11). Taken together these data show that the stimulation of F-actin recruitment to surface-bound phagocytic particles by activated Rac1 is independent of activities of FAK, MerTK, or other protein tyrosine kinases that are inhibited by herbimycin or genistein.

DN-Rac does not affect FAK and MerTK activation in response to phagocytic challenge

The results above and our previous studies show that RPE cells stimulate FAK, MerTK, and Rac1 in an αvβ5 integrin–dependent manner and that inhibition of any of these three proteins abolishes POS engulfment. Since Rac1 activation with POS challenge does not depend on FAK or MerTK, we reasoned that Rac1 may instead act upstream of FAK and MerTK in RPE cells. To test this hypothesis, we compared MerTK and FAK tyrosine phosphorylation levels in RPE-J cells infected to express either β-gal control protein or DN-Rac. Following POS incubation, cells were lysed and phosphotyrosine-containing proteins were isolated by using antiphosphotyrosine beads (PY beads). We found that DN-Rac–expressing RPE-J cells responded to POS challenge by significantly increasing tyrosine phosphorylation of both MerTK and FAK (Figure 12A, PY beads). Changes in phosphorylation of MerTK and FAK were specific to POS challenge, as they did not occur in cells receiving assay medium. Control immunoblots of lysates before bead addition confirmed that protein levels of MerTK, FAK, and Rac1 were similar among all cells tested and that adenoviral infection resulted in efficient expression of β-gal and DN-Rac (Figure 12A, lysate). Statistical analysis confirmed that POS challenge increased phosphotyrosine content of MerTK and of FAK to the same extent in cells expressing β-gal or DN-Rac (Figure 12B). These results demonstrate that activation of FAK and MerTK during POS phagocytosis does not require activation of Rac1.

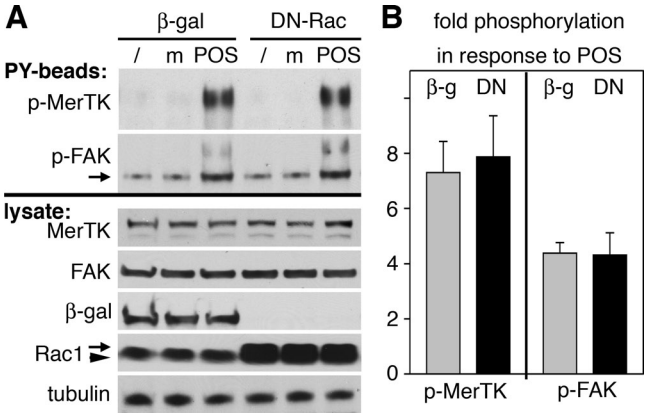

FIGURE 12: FAK and MerTK activation in response to POS challenge are unaffected by DN-Rac. RPE-J cells expressing β-gal or DN-Rac were lysed untreated (/) or after challenge with assay medium (m) or POS for 1 h before isolation of tyrosine-phosphorylated proteins. (A) Top, a representative blotting membrane with PY bead–isolated proteins probed sequentially for MerTK and FAK (as indicated). Bottom, a whole-lysate blot from the same experiment probed sequentially for proteins (as indicated). (B) Bars report relative levels of MerTK and FAK detected on PY-bead blot (p-MerTK and p-FAK, respectively) in cells after POS challenge compared with cells after challenge with assay medium. Bars show mean ± SD fold change determined in three independent experiments, each testing cells expressing β-gal (gray bars) and cells expressing DN-Rac (black bars).

DISCUSSION

This study identifies a critical role specifically for Rac1 in clearance phagocytosis by RPE cells in culture and in intact retinal tissue. To our knowledge, our results are the first to demonstrate Rac1 activity changes in any form of phagocytosis in vivo in intact tissue. Our studies of RPE cells in culture demonstrate that Rac1 activation is essential for engulfment by RPE cells. Furthermore, our experiments provide important new insight into the signaling dependence of Rac1 activation during phagocytosis (summarized in Figure 13).

Lack of Rac1 stimulation with peak POS phagocytosis in $\beta5^{-/-}$ and MFG-$E8^{-/-}$ retina is important in vivo evidence for a dependence of Rac1 and engulfment signaling initiated downstream of αvβ5 integrin ligation. Earlier studies demonstrated that β5 integrin overexpression is sufficient to increase levels of activated Rac1 in resting 293T cells (Albert *et al.*, 2000; Akakura *et al.*, 2004). In this study, we demonstrate that endogenous αvβ5 integrin is required for endogenous Rac1 activation during POS phagocytosis by RPE in culture and in intact retinal tissue.

Our results clearly show that specific inhibition of Rac1 alone is sufficient to prevent F-actin recruitment to sites of surface-bound

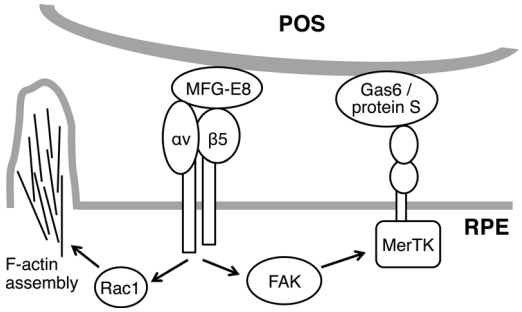

FIGURE 13: POS binding via MFG-E8 to αvβ5 integrin receptors stimulates two cytoplasmic signaling pathways in RPE cells: toward Rac1/F-actin and toward FAK/MerTK. Activation of both pathways is required for engulfment of surface-bound POS.

phagocytic particles in RPE cells. This extends earlier observations showing that inhibition of all Rho family GTPases results in lack of F-actin assembly beneath apoptotic particles recognized in an αvβ3 integrin–dependent manner by bone marrow–derived macrophages (Leverrier and Ridley, 2001). In these cells, expression of dominant-negative Rac1 or Cdc42 partially inhibited particle engulfment. It was not reported whether and which GTPase activity changed upon particle challenge in cells that had not been manipulated pharmacologically or genetically. In our study, we focused on Rac1, guided by our observation that endogenous Rac1 specifically, but not Cdc42 or RhoA, was robustly activated in RPE cells in response to phagocytic particles. Moreover, RPE phagocytosis proceeded normally in the presence of dominant-negative Cdc42 (unpublished data). We conclude that RPE cells exclusively employ Rac1, while macrophages may use both Rac1 and Cdc42 for clearance phagocytosis. Regardless, F-actin recruitment to surface-tethered particles in both αv integrin–dependent forms of phagocytosis does not occur when Rac1 alone is inhibited. In contrast, F-actin assembly beneath opsonized particles bound to immunoglobulin E (IgE)-specific Fc receptors occurs normally in mast cell–derived cells expressing dominant-negative Rac1 (Massol *et al.*, 1998). Although F-actin accumulates to form phagocytic cups in these cells, inhibition of either Rac1 or Cdc42 reduces the number of engulfed particles by about one-half by interfering with phagosome closure. During phagocytosis via IgG-specific Fc receptors (FcγRs), Cdc42 acts upstream of Rac1, as is shown by inhibition of either Cdc42 or Rac1, which effectively stops engulfment and formation of normal phagocytic cups, while allowing some focal F-actin assembly beneath bound particles (Cox *et al.*, 1997; Caron and Hall, 1998). More recently, live-imaging experiments have resolved distinct phases of GTPase activation during FcγR-dependent phagocytosis and have linked recruitment of active Cdc42 and Rac1 and different F-actin changes to early and later phase of particle engulfment, respectively (Hoppe and Swanson, 2004; Beemiller *et al.*, 2010). Furthermore, silencing of Cdc42 is sufficient to reduce FcγR-dependent phagocytosis and eliminate F-actin recruitment to phagocytic particles in macrophages in culture, indicating that endogenous Cdc42 is essential for these processes (Park and Cox, 2009). This study did not reassess the role of Rac1. Taken together these data suggest that Rac1 may participate in distinct steps in different phagocytic mechanisms. Initial F-actin assembly may be regulated differently, depending on the type of particle-binding receptor. We speculate that the cytoplasmic face of the αvβ5 integrin receptor and its associated cytosolic proteins may provide a recruitment site for Rac1, facilitating its contributions to F-actin assembly and, possibly, subsequent steps of the engulfment process. Indeed, our immunofluorescence data show that endogenous Rac1 redistributes early upon POS challenge and may localize to bound and engulfed POS, where it may continue to function.

Unexpectedly, we found that acute, nonspecific inhibition of tyrosine kinase activity by pharmacological inhibitors does not alter the prompt activation of Rac1 and F-actin assembly beneath particles during phagocytosis. The transient stimulation and importance of rapid protein regulation by tyrosine phosphorylation during all forms of phagocytosis is well documented in numerous experimental systems, including the RPE. Tyrosine-phosphorylated proteins colocalize with F-actin phagocytic cups; inhibiting all Rho GTPases prevents cup formation and reduces particle-associated tyrosine phosphorylation (Leverrier and Ridley, 2001). Our results indicate that phagocytic Rac1 activation and F-actin dynamics likely do not require de novo tyrosine phosphorylation upon POS challenge. However, it is possible that resting, differentiated RPE cells possess tyrosine-phosphorylated proteins that participate in F-actin assembly.

Our results showing normal Rac1 activation and recruitment of F-actin to bound POS in RPE cells lacking FAK or MerTK activity are very intriguing. Both in vivo and cell culture experiments have previously demonstrated that engagement of αvβ5 receptors in the RPE by phagocytic particles stimulates associated FAK, resulting in its activation and release, and downstream activation of MerTK (Finnemann, 2003; Nandrot *et al.*, 2004). In this study, we show that Rac1 stimulation of F-actin recruitment during phagocytosis depends on αvβ5 ligation by MFG-E8 like activation of FAK and MerTK. However, F-actin dynamics and these tyrosine kinases are independently activated downstream of αvβ5 in response to POS challenge, such that inhibition of FAK or lack of MerTK does not affect Rac1 or F-actin recruitment and vice versa (Figure 13). FRNK expression preceded the POS phagocytosis assays by many hours, and FAK$^{-/-}$ MEFs and RCS rat RPE entirely and constitutively lack FAK and MerTK, respectively. We thus conclude that neither kinase has a direct role in αvβ5 integrin–dependent signaling pathways promoting Rac1 activation during phagocytosis. Recent work implicates MerTK in recruitment of cytosolic myosin II to bound POS, suggesting a role for MerTK in actin–myosin force generation that likely occurs subsequent to the formation of the F-actin phagocytic cup and that is also important for particle ingestion (Strick *et al.*, 2009). However, it is not clear whether myosin II activation may compensate for MerTK deficiency, and other MerTK signaling targets remain poorly understood. Finally, αvβ5 integrin receptors and FAK reside in a complex whose disruption by FRNK prevents FAK and MerTK activation in response to POS binding by αvβ5 (Finnemann, 2003). Our data showing normal FAK phosphorylation in response to POS in the presence of DN-Rac imply that αvβ5-FAK interactions remain intact under this condition. If Rac1 also associates with the αvβ5 integrin complex, we speculate that this association is unperturbed by FRNK and may rely on distinct cytoplasmic motifs displayed by αvβ5 receptors. Even if Rac1 does not itself reside in a physical complex with αvβ5, its functional dependence on αvβ5 suggests communication from MFG-E8–bound αvβ5 integrin receptors to Rac1, most likely via additional cytoplasmic proteins. Additional studies will be necessary to identify such proteins and the signaling mechanisms that selectively link Rac1 to αvβ5 integrin.

MATERIALS AND METHODS

Reagents

Reagents were purchased from Sigma-Aldrich (St. Louis, MO) or from Invitrogen (Carlsbad, CA) unless otherwise stated.

Animals

All procedures involving animals were performed according to the National Institutes of Health (NIH) *Guide for the Care and Use of*

Laboratory Animals, 8th edition (http://grants.nih.gov/grants/olaw/olaw.htm) and reviewed and approved by the Fordham University Institutional Animal Care and Use Committee. Animals were housed under cyclical 12-h light:12-h dark light conditions and fed ad libitum. $\beta5^{-/-}$ and $\beta5^{+/+}$ wt mice of the same genetic background (129T2/SvEmsJ; Huang *et al.*, 2000; Nandrot *et al.*, 2004, 2006), MFG-$E8^{+/-}$ and MFG-$E8^{-/-}$ mice (Atabai *et al.*, 2005, Nandrot *et al.*, 2007), RCS-rdy/rdy-p rats (MerTK$^{-/-}$), and wt Long-Evans rats (MerTK$^{+/+}$) were bred. For tissue isolation, animals were killed at precise times of day by CO_2 asphyxiation immediately before eyeball enucleation and processing. The cornea and lens were removed before tissue lysis or processing for RPE isolation. For tissue lysis, mice were used at age 6 wk, while rats were used at age 18–20 d.

Antibodies

Primary antibodies to the following proteins were used for this study: β5 integrin, FAK, and RhoA (Santa Cruz Biotechnologies, Santa Cruz, CA); β-gal (Rockland Immunochemicals, Gilbertsville, PA); Cdc42 (raised in mouse; Millipore, Billerica, MA); Cdc42 (raised in rabbit) and Tyro3 (Cell Signaling, Cambridge, MA); opsin (a kind gift from Paul Hargrave, University of Florida, Gainesville, FL; Adamus *et al.*, 1991); MFG-E8 and MerTK (R & D Systems, Minneapolis, MN), Rac1 (BD Biosciences, San Jose, CA), RPE65 (Genetex, Irvine, CA), and α–β-tubulin (Abcam, Cambridge, MA).

Cell culture, toxin and drug treatment, adenoviral infection, and small interfering RNA treatment

RPE-J cells (ATCC, Manassas, VA) were maintained at 32°C and 8% CO_2 in DMEM supplemented with 4% FBS (CELLect Gold; ICN, Irvine, CA) and were subcultured every 7 d. Cells were seeded at 50% confluence and used for experiments 6 d after plating.

RPE cells from 9- to 11-d-old wt and $\beta5^{-/-}$ mice or wt Long-Evans and RCS rats for primary culture were isolated as previously published in detail (Finnemann, 2003; Nandrot *et al.*, 2004). Briefly, the cornea, lens, iris, and vitreous body were removed from freshly enucleated eyes. Eyecups were incubated in 1 mg/ml hyaluronidase in Hank's balanced saline solution (HBSS) without Ca^{2+} and Mg^{2+} for 45–60 min at 37°C. The neural retina was removed, and eyecups were incubated in 2 mg/ml trypsin in HBSS with Ca^{2+} and Mg^{2+} for 30–45 min at 37°C. RPE sheets were manually collected from the underlying choroid. Purified RPE patches were grown in 96-well plates with or without collagen IV–coated glass coverslips in DMEM 10% FBS at 37°C, 5% CO_2 for 5–7 d before experiments. $FAK^{-/-}$ and $FAK^{+/+}$ MEFs originally derived from littermates (CRL-2644 and CRL-2645; ATCC) were grown in 24-well plates in DMEM 10% FBS at 37°C, 5% CO_2 and used at confluence.

To inhibit Rho family GTPases or to inhibit RhoA alone, we incubated cells overnight before experiments with *Clostridium difficile* toxin B (a gift from K. Aktories, University of Freiburg, Germany) at 10 µg/ml or a cell-permeable form of *Clostridium botulinum* C3 transferase (Cytoskeleton, Denver, CO) at 0.25 µg/ml, respectively.

Protein tyrosine kinase inhibitors genistein and herbimycin A (EMD Biosciences, San Diego, CA) were used at 20 µM during select POS phagocytosis assays.

Replication-defective, recombinant adenoviruses encoding β-galactosidase, DN-Rac, (both from Cell Biolabs, San Diego, CA), or FRNK (a gift from D. Schlaepfer, Scripps Research Institute, Lathin spaceJolla, CA) were diluted in serum-free DMEM and applied to polarized RPE-J or primary RPE cells at 5–10 multiplicity of infection overnight for infection. Cells were further incubated for 2 d in complete culture medium before experiments.

To silence Rac1 expression, RPE-J cells were transfected with a mixture of four different 21-nucleotide RNAs specifically targeting rat Rac1 (Accell SMARTpool small interfering RNA [siRNA]; designed and produced by Dharmacon/Thermo Fisher, Lafayette, CO) using Metafectene Pro (Biontex, San Diego, CA) according to the manufacturer's protocols and were used for assays 48 h later. Accell nontargeting siRNA pool (Dharmacon), confirmed to have minimal targeting of known genes in human, mouse, and rat cells, was used as negative control.

POS phagocytosis assays

POS were purified from porcine eyes obtained fresh from a local slaughterhouse according to established procedures (Finnemann *et al.*, 1997). Fluorescent dye labeling was performed by incubating POS for 1 h on a rocker in the dark at room temperature with 0.1 mg/ml FITC (isomer-1) or 0.01 mg/ml Texas Red-X (mixed isomers). Cells in multi-well plates were fed POS at a density of 10 particles/cell in DMEM supplemented with 1.25 µg/ml recombinant mouse MFG-E8 (R & D Systems) for the duration of experiments at 32°C (RPE-J) or 37°C (primary RPE or MEFs), or for 1 h at 20°C to allow only POS binding in pulse–chase experiments (Finnemann and Rodriguez-Boulan, 1999). For experiments comparing TAM and integrin receptor ligands, cells received POS as above or with 1.25 µg/ml recombinant mouse Gas6 (R & D Systems), a mix of 1.25 µg/ml each of MFG-E8 and Gas6, or 5% FBS. After POS pulse, cells were washed three times with phosphate-buffered saline with 0.1 mM $CaCl_2$ and 1 mM $MgCl_2$ (PBS-CM) to remove unbound POS; this was followed by continued incubation at 37°C in DMEM with 5% FBS (chase). All phagocytosis assays were terminated by washing cells three times with PBS-CM. For pulldown assays or quantification of phagocytosed POS by immunoblotting, cells were lysed. If desired, surface-bound POS were selectively removed by incubation in 2 mM EDTA in PBS for 5 min before lysis. Total or internal POS were measured in samples representing equal numbers of RPE cells by quantitative immunoblot detection of opsin, which is exclusive to POS. For quantification of phagocytosed POS by fluorescence scanning, cells were fixed in ice-cold methanol. If desired, FITC fluorescence of surface-bound POS was selectively quenched by incubation in 0.2% trypan blue in PBS-CM for 10 min before fixation. Fluorescence of total or internal FITC-POS was measured by fluorescence scanning using a Typhoon Trio Imager and quantified with ImageQuantTL 7.0 (both from GE Healthcare, Waukesha, WI), as described in detail previously (Finnemann and Rodriguez-Boulan, 1999).

GTPase activity assays

POS phagocytosis assays were performed on RPE cells in 24-well plates as described in *POS phagocytosis assays* and immediately processed precisely according to the manufacturer's instructions using Rac1/Cdc42 or RhoA activation assay kits (Millipore). GTP-loaded and total-sample GTPases were detected by immunoblotting. G-LISA GTPase activity assays (Cytoskeleton) were performed following the manufacturer's instructions on fresh lysates of RPE cells in culture fed with POS or on freshly collected and lysed eyecups. In each experiment, individual samples represented either 1×10^5 RPE cells or two eyecups.

Isolation of tyrosine-phosphorylated proteins

Cells were lysed in HNTG buffer (50 mM HEPES [pH 7.4], 150 mM NaCl, 10% glycerol, 1.5 mM $MgCl_2$, 1% Triton X-100 freshly supplemented with 1% protease and phosphatase-inhibitor cocktails. Clarified lysates representing equal numbers of cells were incubated

with PY beads (P-Tyr-100 antibody-Sepharose bead conjugate; Cell Signaling) for 2 h on a rotator. Beads were washed three times with HNTG buffer before being analyzed by electrophoresis and immunoblotting (see following section).

Protein electrophoresis and immunoblotting

For electrophoretic separation, HNTG lysates representing equal cell numbers or eyecup tissue fractions were boiled for 3 min in reducing SDS sample buffer and separated on SDS–PAGE using standard protocols. Proteins were transferred to nitrocellulose membranes, which were incubated with primary and appropriate horseradish peroxidase–conjugated secondary antibodies followed by enhanced chemiluminescence detection (Perkin Elmer-Cetus, Waltham, MA). X-ray films were scanned and processed using Photoshop CS4 (Adobe, San Jose, CA). Bands were quantified by densitometry using ImageQuant TL 7.0.

Immunofluorescence microscopy

RPE-J cells were fed with fluorescent POS, washed, and fixed with ice-cold methanol. GTPase staining was performed using primary antibodies to Rac1 or RhoA, followed by secondary antibodies conjugated to Alexa Fluor 488. Nuclei were counterstained with 4′,6-diamidino-2-phenylindole.

To costain POS and F-actin, pulse–chase phagocytosis experiments with unlabeled POS were performed using unpassaged primary rat RPE. Cells were fixed with 4% paraformaldehyde in PBS-CM for 20 min and permeabilized with 0.5% Triton-X100 in PBS-CM for 15 min. POS were stained with anti-rhodopsin antibody B6-30 and secondary antibody conjugated to Alexa Fluor 488. F-actin was stained with Alexa Fluor 594–conjugated phalloidin. Images were acquired on a Leica TSP5 laser-scanning confocal microcopy system (Leica, Mannheim, Germany) using sequential scanning mode and were compiled using Photoshop CS4.

Data analysis

Results are presented as mean ± SD. Data were compared using Student's *t* test. Differences with $p < 0.05$ were considered significant.

ACKNOWLEDGMENTS

We thank Kathryn Silva for excellent technical assistance in RPE primary culture preparation. We are grateful to K. Aktories, P. Hargrave, and D. Schlaepfer for generously providing reagents. This work was supported by NIH grant EY013295 from the National Eye Institute (to S.C.F.).

REFERENCES

Adamus G, Zam ZS, Arendt A, Palczewski K, McDowell JH, Hargrave PA (1991). Anti-rhodopsin monoclonal antibodies of defined specificity: characterization and application. Vision Res 31, 17–31.

Akakura S, Singh S, Spataro M, Akakura R, Kim JI, Albert ML, Birge RB (2004). The opsonin MFG-E8 is a ligand for the αvβ5 integrin and triggers DOCK180-dependent Rac1 activation for the phagocytosis of apoptotic cells. Exp Cell Res 292, 403–416.

Albert ML, Kim JI, Birge RB (2000). αvβ5 integrin recruits the CrkII-Dock180-Rac1 complex for phagocytosis of apoptotic cells. Nat Cell Biol 2, 899–905.

Atabai K, *et al*. (2005). MFG-E8 is critical for mammary gland remodeling during involution. Mol Biol Cell 16, 5528–5537.

Beemiller P, Zhang Y, Mohan S, Levinsohn E, Gaeta I, Hoppe AD, Swanson JA (2010). A Cdc42 activation cycle coordinated by PI 3-kinase during Fc receptor-mediated phagocytosis. Mol Biol Cell 21, 470–480.

Bonilha VL, Finnemann SC, Rodriguez-Boulan E (1999). Ezrin promotes morphogenesis of apical microvilli and basal infoldings in retinal pigment epithelium. J Cell Biol 147, 1533–1548.

Caron E, Hall A (1998). Identification of two distinct mechanisms of phagocytosis controlled by different Rho GTPases. Science 282, 1717–1721.

Chaitin MH, Hall MO (1983). The distribution of actin in cultured normal and dystrophic rat pigment epithelial cells during the phagocytosis of rod outer segments. Invest Ophthalmol Vis Sci 24, 821–831.

Cox D, Chang P, Zhang Q, Reddy PG, Bokoch GM, Greenberg S (1997). Requirements for both Rac1 and Cdc42 in membrane ruffling and phagocytosis in leukocytes. J Exp Med 186, 1487–1494.

Dupuy AG, Caron E (2008). Integrin-dependent phagocytosis: spreading from microadhesion to new concepts. J Cell Sci 121, 1773–1783.

Edwards RB, Flaherty PM (1986). Increased phagocytosis of outer segments in the presence of serum by cultured normal, but not dystrophic, rat retinal pigment epithelium. J Cell Physiol 127, 293–296.

Edwards RB, Szamier RB (1977). Defective phagocytosis of isolated rod outer segments by RCS rat retinal pigment epithelium in culture. Science 197, 1001–1003.

Erwig LP, Henson PM (2008). Clearance of apoptotic cells by phagocytes. Cell Death Differ 15, 243–250.

Feng W, Yasumura D, Matthes MT, LaVail MM, Vollrath D (2002). Mertk triggers uptake of photoreceptor outer segments during phagocytosis by cultured retinal pigment epithelial cells. J Biol Chem 277, 17016–17022.

Finnemann SC (2003). Focal adhesion kinase signaling promotes phagocytosis of integrin-bound photoreceptors. EMBO J 22, 4143–4154.

Finnemann SC, Bonilha VL, Marmorstein AD, Rodriguez-Boulan E (1997). Phagocytosis of rod outer segments by retinal pigment epithelial cells requires αvβ5 integrin for binding but not for internalization. Proc Natl Acad Sci USA 94, 12932–12937.

Finnemann SC, Rodriguez-Boulan E (1999). Macrophage and retinal pigment epithelium phagocytosis: apoptotic cells and photoreceptors compete for αvβ3 and αvβ5 integrins, and protein kinase C regulates αvβ5 binding and cytoskeletal linkage. J Exp Med 190, 861–874.

Hoppe AD, Swanson JA (2004). Cdc42, Rac1, and Rac2 display distinct patterns of activation during phagocytosis. Mol Biol Cell 15, 3509–3519.

Huang X, Griffiths M, Wu J, Farese RV, Jr., Sheppard D (2000). Normal development, wound healing, and adenovirus susceptibility in β5-deficient mice. Mol Cell Biol 20, 755–759.

Leverrier Y, Ridley AJ (2001). Requirement for Rho GTPases and PI 3-kinases during apoptotic cell phagocytosis by macrophages. Curr Biol 11, 195–199.

Massol P, Montcourrier P, Guillemot JC, Chavrier P (1998). Fc receptor-mediated phagocytosis requires Cdc42 and Rac1. EMBO J 17, 6219–6229.

Nakaya M, Tanaka M, Okabe Y, Hanayama R, Nagata S (2006). Opposite effects of Rho family GTPases on engulfment of apoptotic cells by macrophages. J Biol Chem 281, 8836–8842.

Nandrot EF, Anand M, Almeida D, Atabai K, Sheppard D, Finnemann SC (2007). Essential role for MFG-E8 as ligand for αvβ5 integrin in diurnal retinal phagocytosis. Proc Natl Acad Sci USA 104, 12005–12010.

Nandrot EF, Anand M, Sircar M, Finnemann SC (2006). Novel role for αvβ5 integrin in retinal adhesion and its diurnal peak. Am J Physiol Cell Physiol 290, C1256–C1262.

Nandrot EF, Kim Y, Brodie SE, Huang X, Sheppard D, Finnemann SC (2004). Loss of synchronized retinal phagocytosis and age-related blindness in mice lacking αvβ5 integrin. J Exp Med 200, 1539–1545.

Park H, Cox D (2009). Cdc42 regulates Fc gamma receptor-mediated phagocytosis through the activation and phosphorylation of Wiskott-Aldrich syndrome protein (WASP) and neural-WASP. Mol Biol Cell 20, 4500–4508.

Prasad D, Rothlin CV, Burrola P, Burstyn-Cohen T, Lu Q, Garcia de Frutos P, Lemke G (2006). TAM receptor function in the retinal pigment epithelium. Mol Cell Neurosci 33, 96–108.

Ridley AJ, Paterson HF, Johnston CL, Diekmann D, Hall A (1992). The small GTP-binding protein rac regulates growth factor-induced membrane ruffling. Cell 70, 401–410.

Schaller MD, Borgman CA, Parsons JT (1993). Autonomous expression of a noncatalytic domain of the focal adhesion-associated protein tyrosine kinase pp125FAK. Mol Cell Biol 13, 785–791.

Sieg DJ, Hauck CR, Schlaepfer DD (1999). Required role of focal adhesion kinase (FAK) for integrin-stimulated cell migration. J Cell Sci 112, 2677–2691.

Strick DJ, Feng W, Vollrath D (2009). Mertk drives myosin II redistribution during retinal pigment epithelial phagocytosis. Invest Ophthalmol Vis Sci 50, 2427–2435.

Tosello-Trampont AC, Brugnera E, Ravichandran KS (2001). Evidence for a conserved role for CRKII and Rac in engulfment of apoptotic cells. J Biol Chem 276, 13797–13802.

Wu Y, Singh S, Georgescu MM, Birge RB (2005). A role for Mer tyrosine kinase in αvβ5 integrin-mediated phagocytosis of apoptotic cells. J Cell Sci 118, 539–553.